

A Study of the Parameters That Effect the Quality of the Estimated Modal Parameters in Automated Enhanced Frequency Domain Decomposition Algorithm

Muhammad Danial Bin Abu Hasan^{1*}, Zair Asrar Bin Ahmad²,
Mohd Salman Leong¹ and Lim Meng Hee¹

¹*Institute of Noise and Vibration, Universiti Teknologi Malaysia, 54100 UTM, Kuala Lumpur, Malaysia*
²*School of Mechanical Engineering, Universiti Teknologi Malaysia, 81310 UTM, Skudai, Johor Bahru, Malaysia*

ABSTRACT

This paper presents parameters analysis for the estimated modal damping ratio using a new version of the automated enhanced frequency domain decomposition (AEFDD). The purpose of this study is to provide a better choice of a maximum number of points of time segments and modal assurance criterion (MAC) index number regarding to the variable level of system damping (low and high damped structure) and degree of freedom of the system. According current literature, frequency domain (FD) methods seem to have the problem with providing a correct identification of the modal damping ratio, since the correct estimate of modal damping is still an open problem and often leads to biased estimates. This technique is capable of providing consistent modal parameters estimation, particularly

for modal frequencies and mode shapes. As a necessary fundamental condition, the algorithm has been assessed first from computed numerical responses according to random white noise, acting on different shear-type frame structures and corrupted with noise. Results indicate that reducing the value of natural frequencies and modal damping ratios of the modes under analysis demands longer time segments and a high value of the maximum number of points for adequate information on the decaying

ARTICLE INFO

Article history:

Received: 6 February 2020

Accepted: 14 May 2020

Published: 16 July 2020

E-mail addresses:

muhd_danial200@yahoo.com (Muhammad Danial Bin Abu Hasan)

zair@utm.my (Zair Asrar Bin Ahmad)

salman.leong@gmail.com (Mohd Salman Leong)

limmenghee@gmail.com (Lim Meng Hee)

*Corresponding author

correlation functions when computing a modal damping ratio. In addition, the results also prove that the MAC index does not significantly affect the results for the low damped system. However, the use of a high MAC index value for the high damped system significantly introduces large error bound and it becomes worse, particularly for the higher modes, as the standard deviation of percentage error increases gradually. Furthermore, the use of a MAC index for a high number of points of time segments significantly increases the standard deviation of the percentage error.

Keywords: Automated OMA, automatization, frequency domain decomposition, operational modal analysis

INTRODUCTION

The present structural modal identification method, operational modal analysis (OMA) is widely and normally used within various engineering fields due to its ability to perform cost-effective and fast tests that depend solely on structural response signals generated by ambient excitations without affecting its operating conditions (Rainieri & Fabbrocino, 2015). This means that OMA techniques have major advantages compared to classical experimental modal analysis (EMA), which requires input excitations for structural modal identification (Mironov et al., 2015; Zhang et al., 2005). In the literature, the classical frequency domain decomposition (FDD) was originally proposed by Brincker et al. (2001a) and this technique is based on the singular value decomposition (SVD) of the power spectral density (PSD) matrix of the response signals (Brincker et al., 2001b; Gade et al., 2005). With simple execution and user-friendly characteristics, this technique is also capable of providing consistent modal parameters estimation, particularly for modal frequencies and mode shapes; however, modal damping value was not clarified in their work. Later, the second generation of FDD, known as enhanced frequency domain decomposition (EFDD), was introduced to enhance the accuracy of modal frequencies and explain how to estimate modal damping ratios (Brincker et al., 2001a). The third generation of FDD, frequency-spatial domain decomposition (FSDD), was proposed in the following years to overcome some problems in EFDD algorithms (Brincker & Zhang, 2009; Wang et al., 2005; Zhang et al., 2010). According to the existing literature, frequency domain (FD) methods are capable of detecting modal frequencies and mode shapes in terms of closely spaced modes or even repeated modes, since SVD can isolate the signal from noise (Zhang & Tamura, 2003). However, frequency domain (FD) methods seem to have the problem of providing a correct identification of the modal damping ratio, since the actual estimation of modal damping is still an open problem and frequently leads to biased estimates, although natural frequencies and mode shapes can be estimated confidently (Rainieri & Fabbrocino, 2014; Rainieri & Fabbrocino, 2015).

Most of the researchers have tried to improve modal damping estimation by introducing a variety of techniques for modal damping estimation in FDD-type procedures such as logarithmic decrement (LogDec) method (Brincker et al., 2001a; Gade et al., 2005), Hilbert transform (HT) (Zhang & Tamura, 2003), natural excitation techniques (NExt) ie cross-covariance function, Ibrahim time domain, and Polyreference (Bajrić et al., 2015a) as well as the optimal wavelet (Tarinejad & Damadipour, 2014). Furthermore, a new approach involving hybrids or combinations of two methods together is also introduced to improve modal damping estimation such as Enhanced FDD Algorithm in-operation modal appropriation (EFDD-INOPMA) (Ghalishooyan et al., 2019), Frequency Domain Decomposition-Natural Excitation Technique (FDD-NExT) (Frans & Arfiadi, 2019), Frequency Domain State Space-Based Mode Decomposition Framework (Hwang et al., 2019) and Frequency Domain Stochastic Subspace Identification (Chou & Chang, 2020). However, this issue is still considered as an open problem, even though some researchers have also tried to tackle the signal processing issue by making improvements using their proposed method since, the signal processing also denoted as the contributing factor for estimation errors comprising estimates of correlation function (CF) and the spectral density (SD) (Bajric et al., 2015b). After throughout critical reviews and pilot tests, there is another factor that contributes to this error which is caused by parameter extraction, particularly in term of proper selection of the correct time window, extrema picking of single degree of freedom (SDOF) auto-correlation function and modal assurance criterion (MAC) index selection which turn out to be the most challenging part of the algorithm. Time window, extrema picking of SDOF auto-correlation function and MAC index selection need to be carefully chosen, otherwise it will lead to random and bias errors. Therefore, particular attention is needed for proper selection of the correct time window, MAC index selection and extrema picking of a single degree of freedom (SDOF) auto-correlation function. Currently, some researchers have tried to address this problem by introducing iterative loop optimization in the selection of the correct time window, extrema picking of single degree of freedom (SDOF) auto-correlation function and MAC index selection. The refined FDD is a new version of EFDD. However, they can only improve the estimation of modal damping ratios up to 75% and 95% for the natural frequencies but ineffective for a very high noise and only reported for the high damped system (Brincker et al., 2001b; Pioldi et al., 2016; Pioldi et al., 2017; Pioldi & Rizzi, 2015; Pioldi & Rizzi, 2017; Pioldi & Rizzi, 2018; Pioldi et al., 2014).

The proposed method which is an automated EFDD method tried to improvise the recent method, Refined FDD by introducing a new approach of iterative loop optimization in the selection of the correct time window and extrema picking of single degree of freedom (SDOF) auto-correlation function. Meanwhile for MAC index selection, further analysis is needed to identify the appropriate range of MAC index value for a different level of system

damping (low and high damped structure) because the study on refined FDD is limited to the high damped structure only.

Therefore, the purpose of this study is to evaluate the performance of the automated version of the EFDD method by performing parameter analysis for the estimated modal damping ratio to provide a better choice of a maximum number of points of time segments and modal assurance criterion (MAC) index number regarding the variable level of system damping (low and high damped structure) and degree of freedom of the system.

MATERIALS AND METHODS

All the frequency domain methods in OMA share similar characteristics in terms of the spectral density (SD) function assessment from the output responses, but each of them has a different way of extracting structural modal parameters. Further information on the automated EFDD method algorithm is discussed in this section.

The overall schematic illustration of the automated EFDD method procedure is shown in Figure 1. At first, each method in OMA including the FD method is required to go through signal processing before the modal identification process takes place. This is because all the modal information generally is suppressed in the mess made by the randomness of the measured signals. Thus, signal processing is used to provide a clearer picture of the physical problem being dealt with. Signal processing consists of correlation functions (CF) and spectral densities (SD) function. The CF matrix was estimated using the direct method, as given by Equation 1.

$$\hat{R}(k) = (1/(N - k))Y_{(1:N-k)}Y^T_{(k+1:N)} \quad (1)$$

Where the measured responses are arranged as a column in data series, N is the total number of data points in the time series, k corresponds to the time lag $\tau = k\Delta t$ and $(N - k)\Delta t$ corresponds to $T - \tau$, T is the total length of the time series. Before estimating SD, the fast Fourier transform (FFT) algorithm requires time windows to reduce leakage by forcing the endpoints of each signal sample data to zero. In this study, the flat-triangular window with $\alpha = 0.5$ was chosen. Next, the singular value decomposition (SVD) is applied to decompose the output SD into auto SD that represents an SDOF system. The singular value data that are identified around a resonance peak by using modal assurance criterion (MAC) filtering, which is also known as spectral bell identification (Gade et al., 2005; Zhang & Tamura, 2003), are transferred back to the time domain (TD) using the inverse FFT (Gade et al., 2005; Zhang & Tamura, 2003).

Considering two different vectors φ_r and φ_s , that are to be considered as two different estimates of the same experimental mode shape vector (Bricker & Venture, 2015), we can calculate the correlation between the two vectors according to the MAC normally formulated as in Equation 2:

$$MAC(\{\varphi_r\}\{\varphi_s\}) = \frac{|\{\varphi_r\}^{*t}\{\varphi_s\}|^2}{(\{\varphi_r\}^{*t}\{\varphi_r\})(\{\varphi_s\}^{*t}\{\varphi_s\})} \quad (2)$$

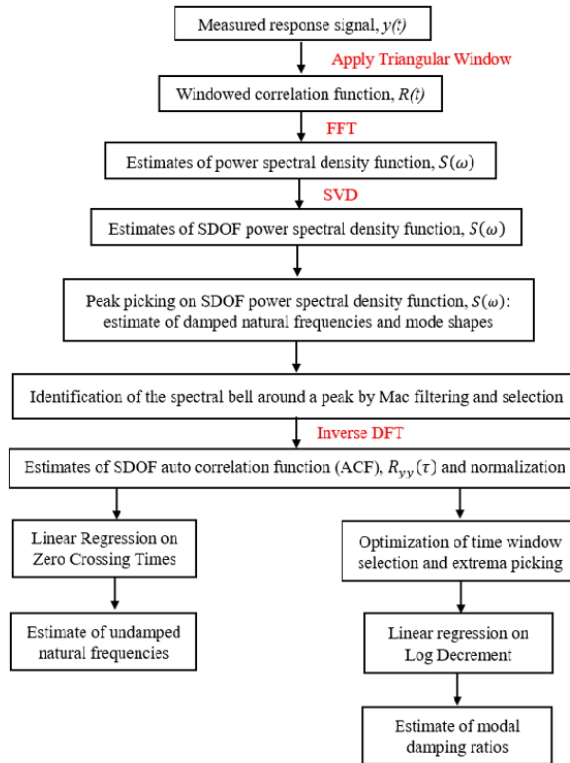


Figure 1. Schematic illustration of FDD procedure

If a linear relationship exists (i.e., the vectors move the same way) between the two complex vectors, the MAC value will be near to one. If they are linearly independent, the MAC value will be small (near zero).

Then, all extrema of the free decay that within an appropriate time window were used to implement the subsequent linear regression operations for assessing the logarithmic decrement (LogDec), δ as characterized in Equation 3 and Equation 4 below:

$$\delta = \frac{2}{k} \ln \left(\frac{r_0}{|r_k|} \right) \tag{3}$$

$$2 \ln(|r_k|) = 2 \ln(r_0) - \delta k \tag{4}$$

where k is an integer counter of the k th extreme of the auto-correlation function, $k = 1, 2, 3, \dots$, while r_0 and r_k are the initial and the k th extreme value of the auto-correlation function, respectively. Then, modal damping ratio can be obtained in Equation 5.

$$\zeta_q = \frac{\delta_q}{\sqrt{4\pi^2 + \delta_q^2}} \tag{5}$$

Meanwhile, the damped natural frequency, ω_d was estimated by linear regression on the zero-crossing times of the equivalent SDOF correlation function. Then, the undamped

natural frequency, ω_n was computed by using the following Equation 6:

$$\omega_n = \frac{\omega_d}{\sqrt{1 - \zeta^2}} \tag{6}$$

Further information on all alternative FD methods can be found in (Jacobsen et al., 2008; Pioldi et al., 2016; Rodrigues et al., 2004).

Validation with Numerical Simulations

As a fundamentally necessary condition, the algorithm had been assessed first from computed numerical responses according to random white noise, acting on different ideal shear-type frame structures. The proposed algorithms were validated via simulated data from a series of multi-storey shear-type models consisting of two, three and six degrees of freedom (DOF) as illustrated in Figure 2. All these structural features with different DOFs are examined first (Zanchi, 2011; Pioldi, 2012; Pioldi, 2013).

The characteristics of the simulated multi-storey shear-type models which present well-separated modes are provided in Figure 3 by the stiffness (K), mass (M) and damping (C) matrices.

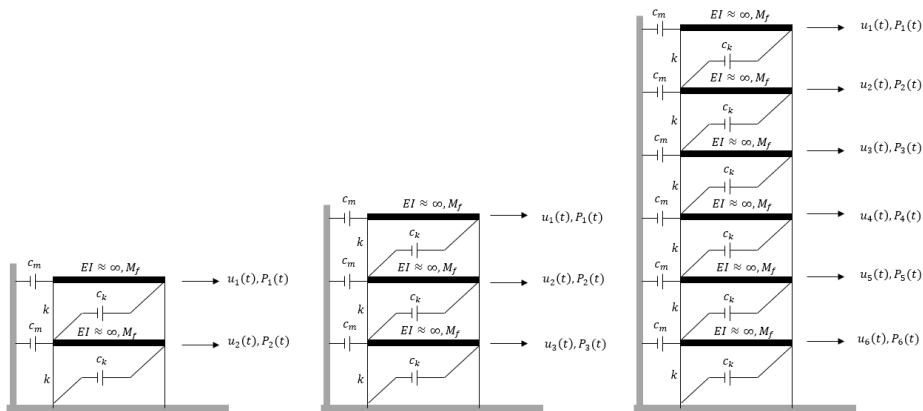


Figure 2. Two-, three and six -storey frame models.

The well-separated modes and different DOFs were used in this study to discover the efficiency of the proposed approach for the diversity of features and type of structure. The system matrices were defined with to achieve modal parameters with values of the same order of magnitude as the ones generally found in present civil engineering structures. Mass and stiffness matrices were set fixed for every frame as reported below. Damping matrices have been assumed to be diagonal in modal coordinates and represented by different modal damping ratios in the numerical tests. The damping of the structure is viscous (damping forces proportional to velocity) and proportional Rayleigh damping, the prescribed modal damping ratios for multi-storey shear-type models are set to $\zeta_k = \zeta_j = 1\%, 3\%$ and 5% of critical damping which consists of low and high values of damping in a structure. In the

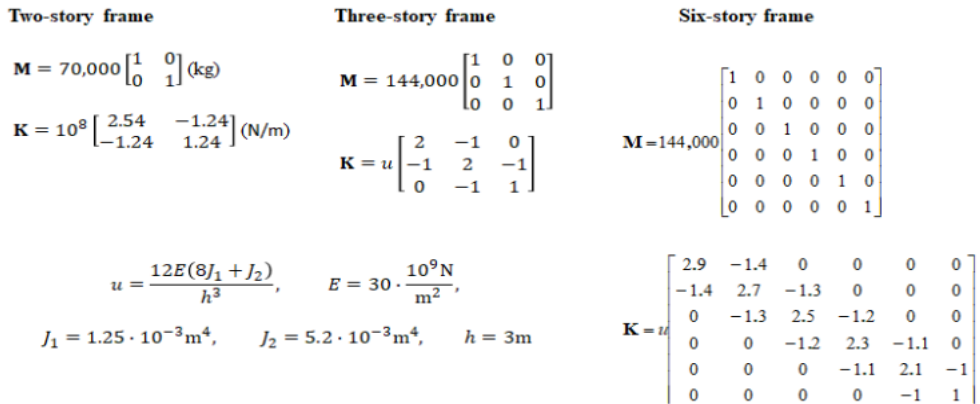


Figure 3. Dynamic system models: the main features of ideal shear-type frames.

literature, only lightly damped structures that contain modal damping ratios below 2% are considered for analysis (Brewick & Smyth, 2013; Brincker et al., 2001a; Brincker et al., 2001b; Gade et al., 2005; Magalhães et al., 2010; Zhang & Tamura, 2003). Input is taken as a stationary broadband ambient excitation with normally distributed random numbers assuming independent inputs for all DOF of the models. It has a constant PSD which can cover a wide range of frequencies and is adequate to excite all the structural modes. The random input excitation, which is also known as zero-mean Gaussian white noise, takes the assumption of the excitation system to be linear and time-invariant. The response of the system was simulated using Newmark’s method with constant average acceleration (i.e. $\gamma=12$ and $\beta=14$) (Chopra, 2001). The adopted parameters in the analysis are shown in Table 1.

The simulated outputs, which are time series with the accelerations of all the DOFs of the models, are corrupted with noise that mimics the influence of the sensors and measuring chain noise. This was simulated by normally distributed random numbers with a standard deviation equal to 10% of the standard deviation of the simulated outputs [this percentage of noise is quite conservative in the case of well-conducted ambient vibration tests (Magalhães, 2010)]. In this numerical simulation, the eigenvalue problem analysis was

Table 1
The adopted parameters for the multi-storey frame in the processing

| Parameters | Two-storey frame | Three-storey frame | Six-storey frame |
|---|------------------|--------------------|------------------|
| Length of time series, $t(\text{s})$ | 400 | 600 | 1000 |
| Sampling frequency, $f_s(\text{Hz})$ | 200 | 200 | 200 |
| Adopted frequency resolution, $\Delta f(\text{Hz})$ | 0.0025 | 0.00167 | 0.001 |

used to validate the effectiveness of the proposed approach. By taking the values of the stiffness K , mass M , and damping C , the modal parameters (modal damping ratio, natural frequency and mode shape) can be estimated.

The automated version of the EFDD method was tested on multi-storey shear-type models which consisted of two, three and six DOF and different levels of damping (1%, 3% and 5% of critical damping, which consisted of low and high damped systems) with the appropriate variation of the MAC index ranging from 0.70 to 0.99 based on a literature review (Pioldi et al., 2016) and using ten alternative time segment lengths that led to spectra with different frequency resolution. Table 2 characterises 70 scenarios (named from 1a to 10g) that involved varying the maximum number of points considered in the time segments from 1024 to 10240 and using a variation of the MAC index that ranges from 0.70 to 0.99. The 70 scenarios are the percentage deviation (error) of estimate modal damping ratios.

The use of multi-storey shear-type models for this analysis requires a large number of simulations and datasets and forced the use of an automated procedure, which is presented in the last section. The automated version of the EFDD method is a robust procedure and adequate for this particular application.

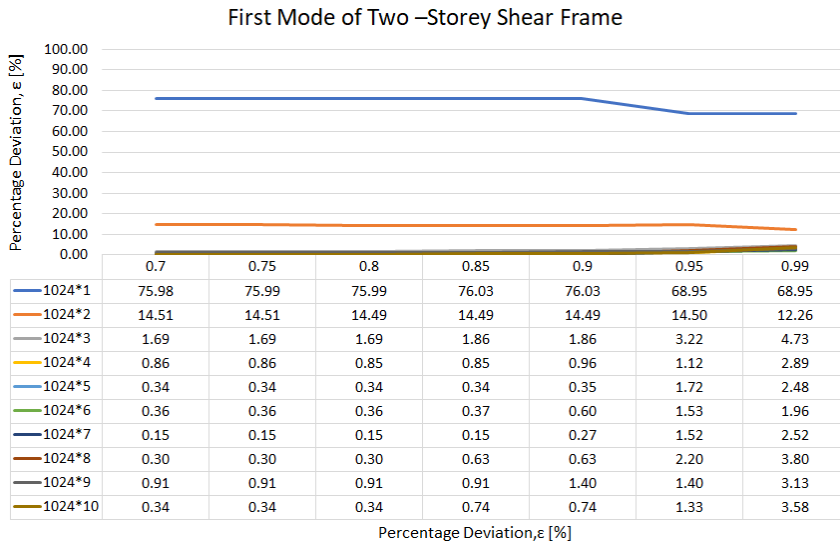
Table 2
Scenarios for the application of the FDD method

| Maximum number of points in the time segments | MAC Index | | | | | | |
|---|-----------|------|------|------|------|------|------|
| | 0.70 | 0.75 | 0.80 | 0.85 | 0.90 | 0.95 | 0.99 |
| 1024*1 | 1a | 1b | 1c | 1d | 1e | 1f | 1g |
| 1024*2 | 2a | 2b | 2c | 2d | 2e | 2f | 2g |
| 1024*3 | 3a | 3b | 3c | 3d | 3e | 3f | 3g |
| 1024*4 | 4a | 4b | 4c | 4d | 4e | 4f | 4g |
| 1024*5 | 5a | 5b | 5c | 5d | 5e | 5f | 5g |
| 1024*6 | 6a | 6b | 6c | 6d | 6e | 6f | 6g |
| 1024*7 | 7a | 7b | 7c | 7d | 7e | 7f | 7g |
| 1024*8 | 8a | 8b | 8c | 8d | 8e | 8f | 8g |
| 1024*9 | 9a | 9b | 9c | 9d | 9e | 9f | 9g |
| 1024*10 | 10a | 10b | 10c | 10d | 10e | 10f | 10g |

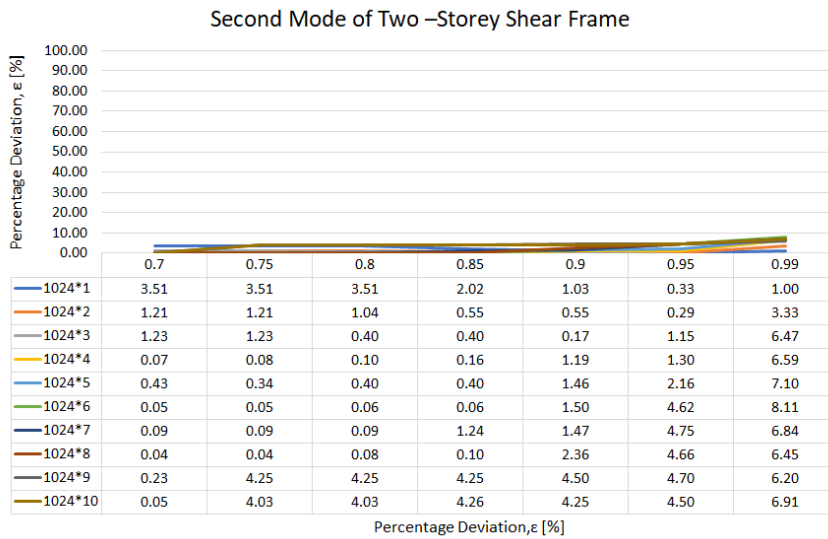
RESULTS AND DISCUSSION

Low Level of Damping (1%)

Percentage deviations (errors) of modal damping ratio for the low damped of two, three and six-storey frame (1%) are shown in Figures 4, 5 and 6.

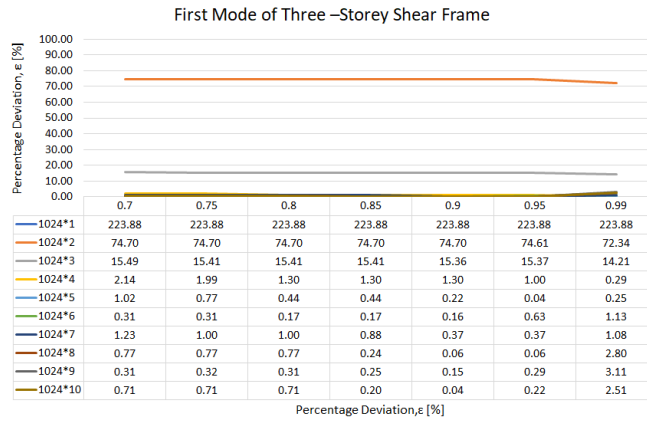


(a)

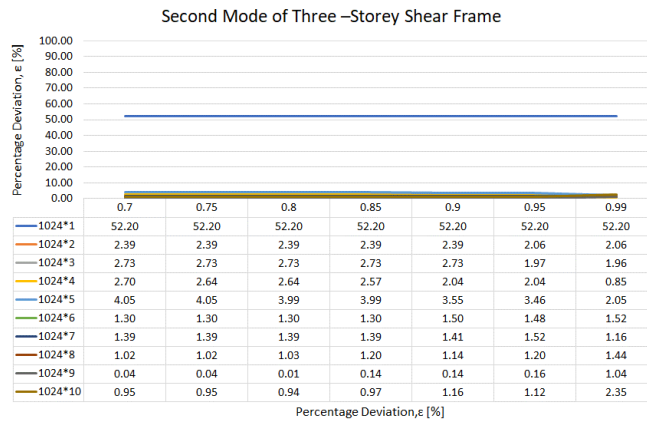


(b)

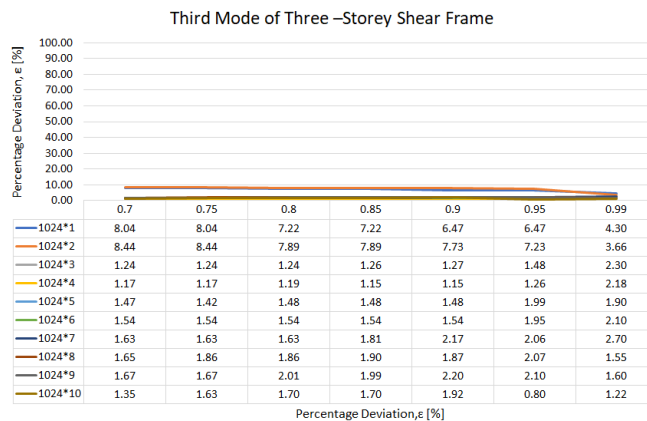
Figure 4. Percentage deviation (error) of modal damping ratio for the low damped two-storey frame (1%): (a) the first mode; (b) the second mode.



(a)



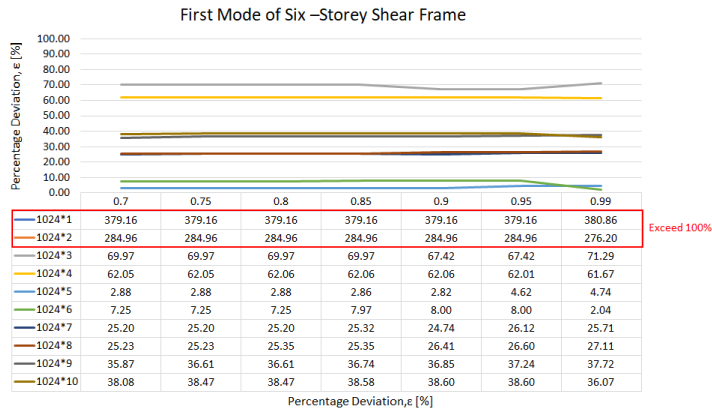
(b)



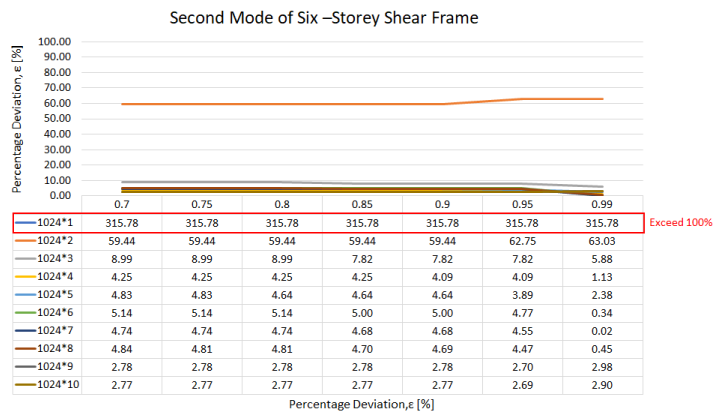
(c)

Figure 5. Percentage deviation (error) of modal damping ratio for the low damped three-storey frame (1%): (a) the first mode; (b) the second mode; (c) the third mode.

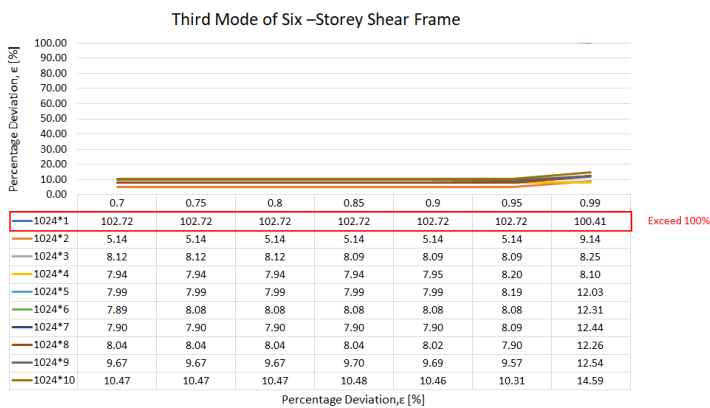
Parameters Study That Effect the Estimated Modal Parameters



(a)

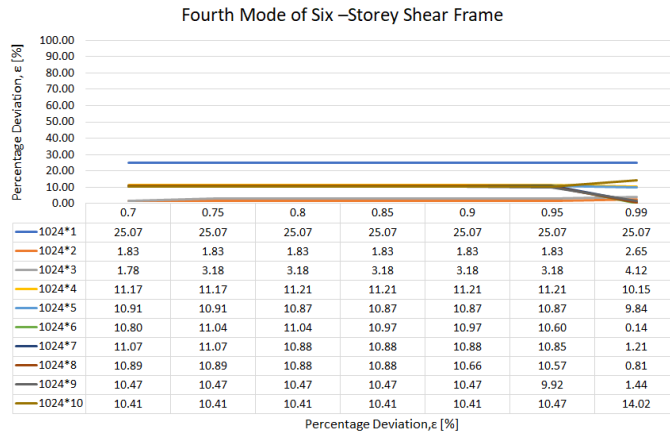


(b)

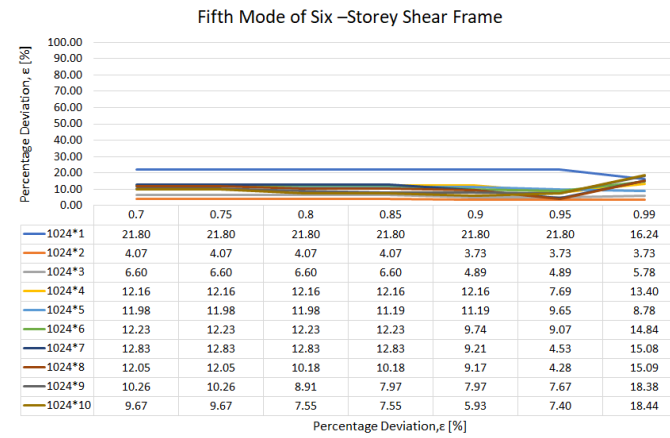


(c)

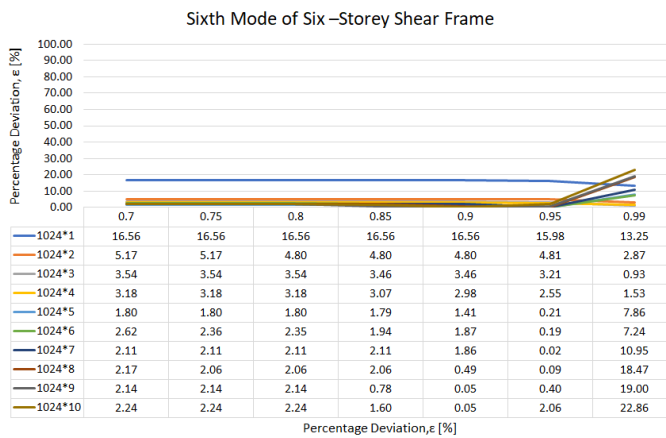
Figure 6. Percentage deviation (error) of modal damping ratio for the low damped six-storey frame (1%): (a) the first mode; (b) second mode; (c) the third mode



(d)



(e)

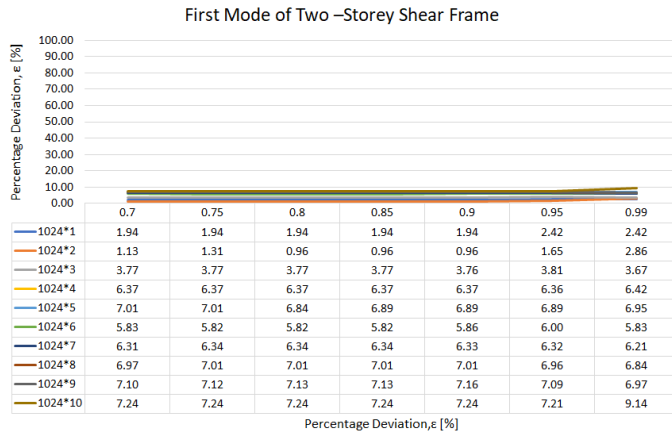


(f)

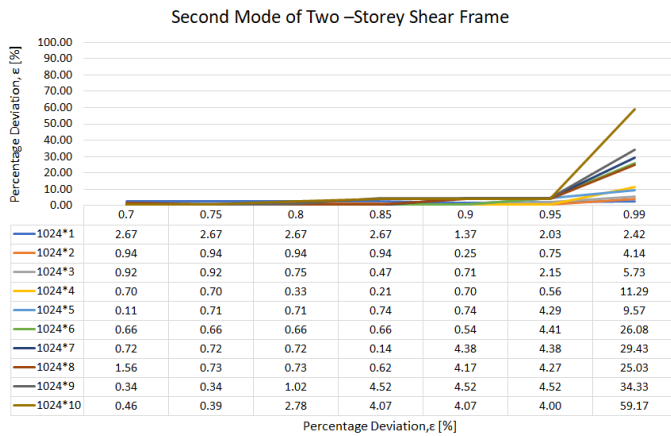
Figure 6. Percentage deviation (error) of modal damping ratio for the low damped six-storey frame (1%): (d) the fourth mode; (e) the fifth mode; (f) the sixth mode.

High Level of Damping (3%)

Percentage deviations (errors) of modal damping ratio for the high damped of two, three and six-storey frame (3%) are shown in Figures 7, 8 and 9.

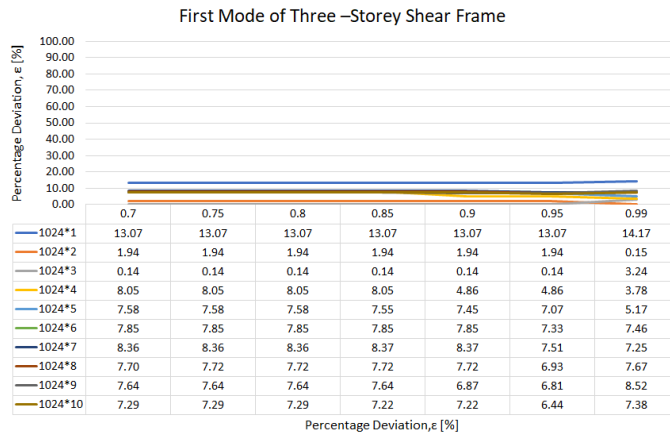


(a)

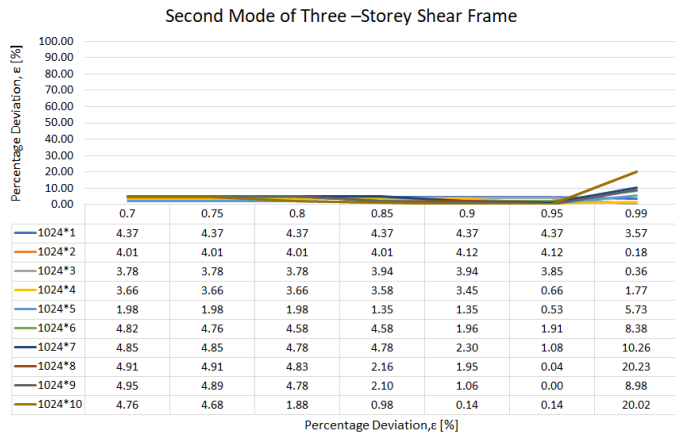


(b)

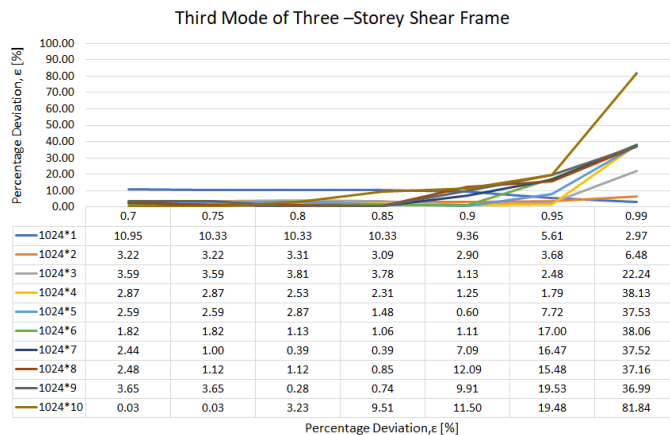
Figure 7. Percentage deviation (error) of modal damping ratio for the high damped two-storey frame (3%); (a) the first mode; (b) the second mode.



(a)



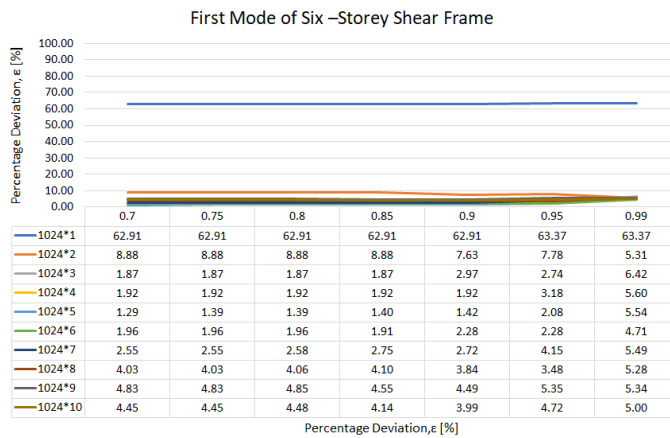
(b)



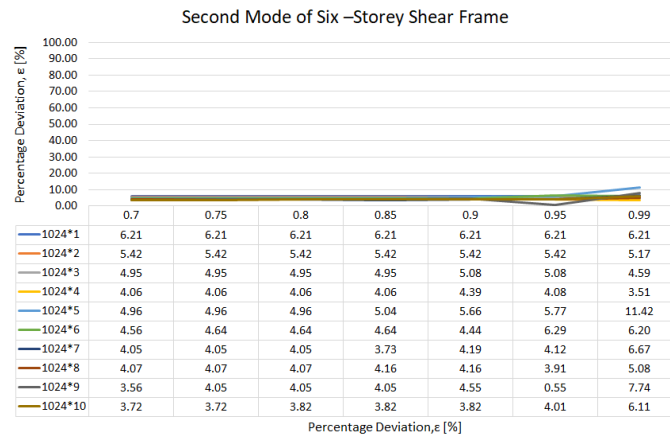
(c)

Figure 8. Percentage deviation (error) of modal damping ratio for the high damped three-storey frame (3%): (a) the first mode; (b) the second mode; (c) the third mode.

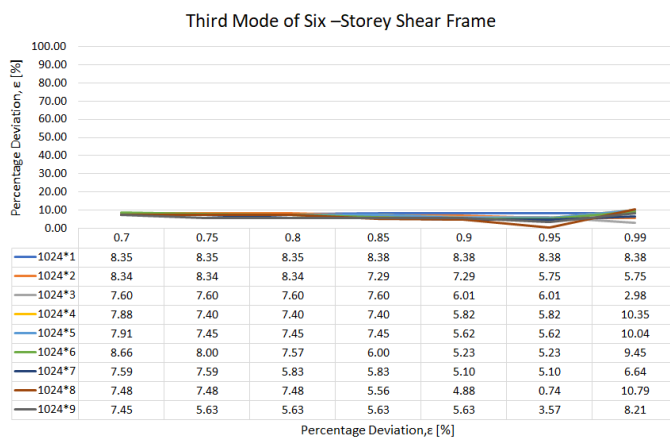
Parameters Study That Effect the Estimated Modal Parameters



(a)

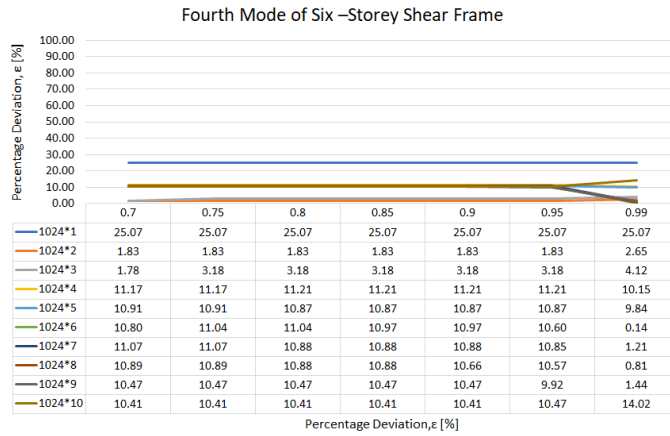


(b)

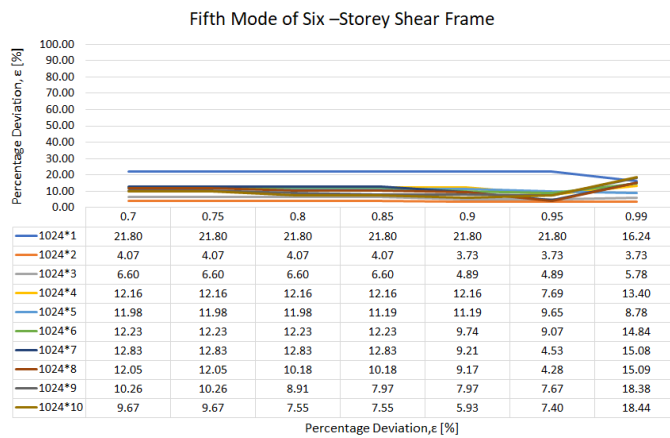


(c)

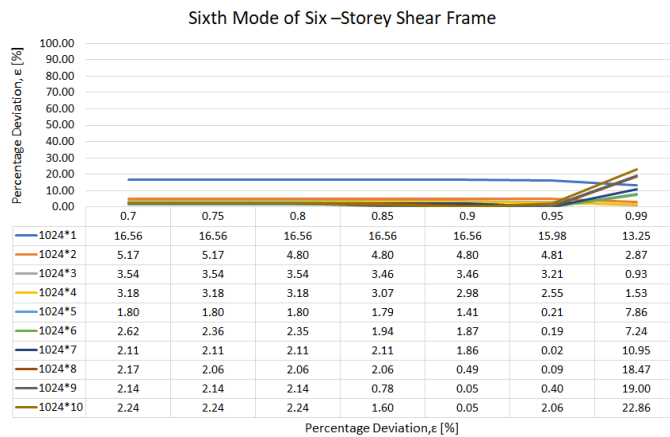
Figure 9. Percentage deviation (error) of modal damping ratio for the high damped six-storey frame (3%): (a) the first mode; (b) second mode; (c) the third mode



(d)



(e)



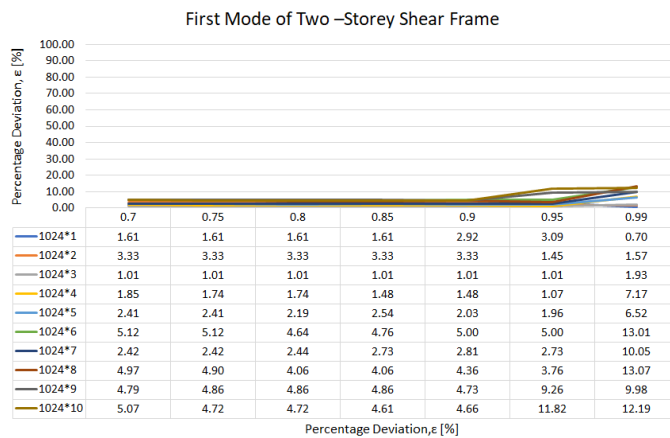
(f)

Figure 9. Percentage deviation (error) of modal damping ratio for the high damped six-storey frame (3%): (d) the fourth mode; (e) the fifth mode; (f) the sixth mode.

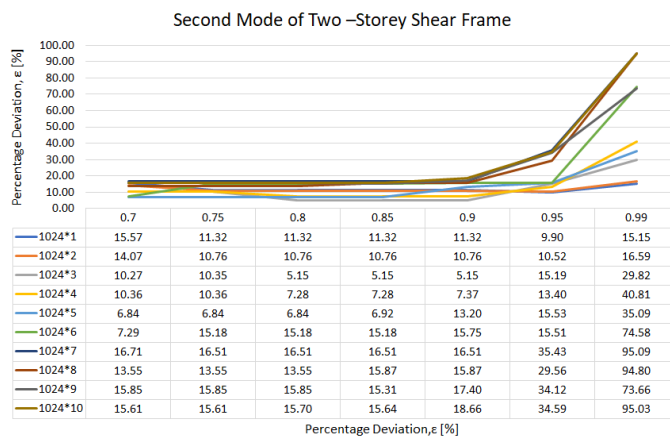
High Level of Damping (5%)

Percentage deviations (errors) of modal damping ratio for the high damped of two, three and six-storey frame (5%) are shown in Figures 10, 11 and 12.

This analysis reveals that a maximum number of points of the time segment or frequency resolution play a major role in presenting high bias results (sometimes above 100%) in cases when this parameter is not well chosen. The frequency resolution and the correct choice of the number of points of the time segments are both interrelated; increasing the number of points means increasing the frequency resolution. The biased estimate of the modal damping ratio is influenced by estimated auto-correlation. The correct selection of a maximum number of time segments for estimating auto-correlation should require some points after the disappearance of the decay to ensure that the length of the estimated

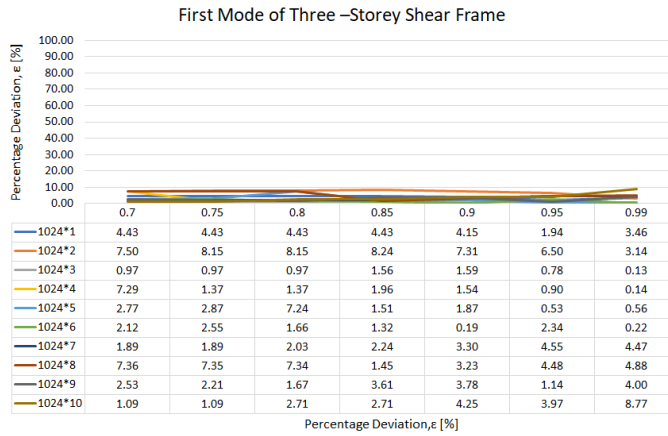


(a)

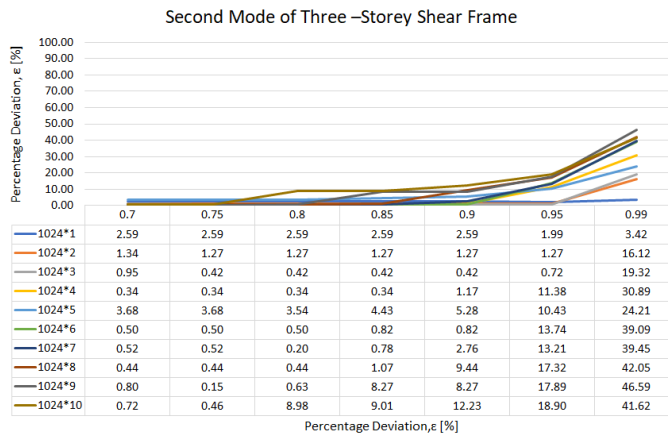


(b)

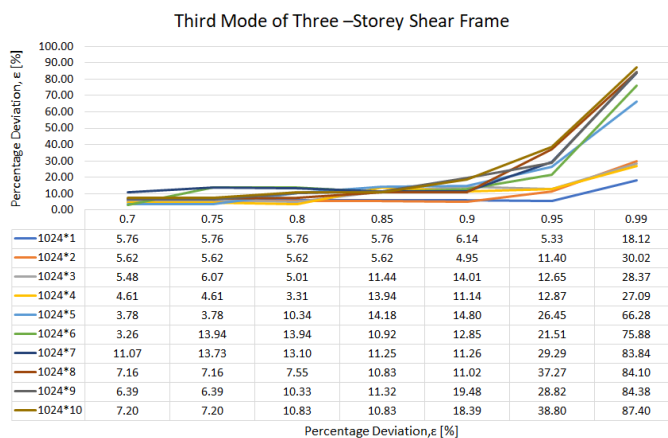
Figure 10. Percentage deviation (error) of modal damping ratio for the high damped two-storey frame (5%): (a) the first mode; (b) the second mode.



(a)



(b)

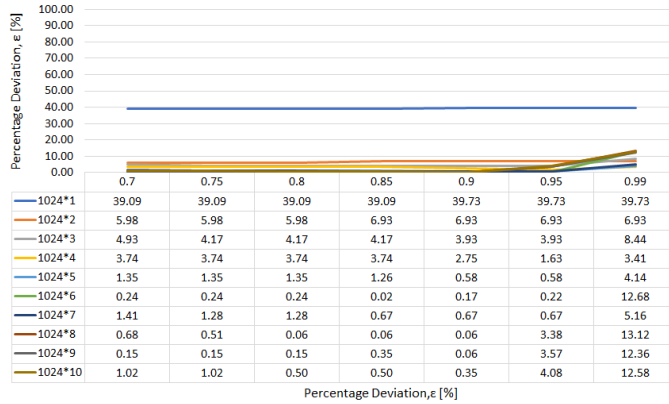


(c)

Figure 11. Percentage deviation (error) of modal damping ratio for the high damped three-storey frame (5%): (a) the first mode; (b) the second mode; (c) the third mode.

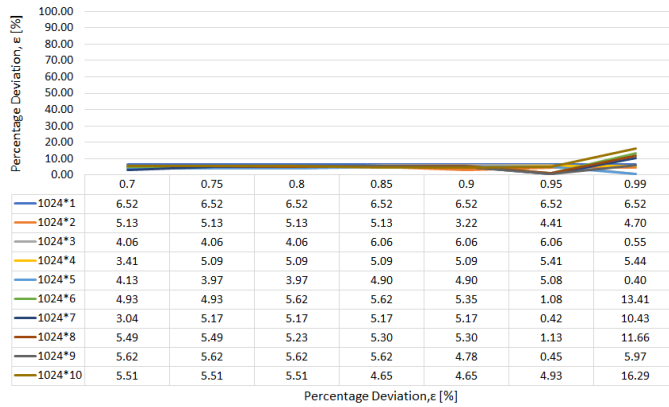
Parameters Study That Effect the Estimated Modal Parameters

First Mode of Six –Storey Shear Frame



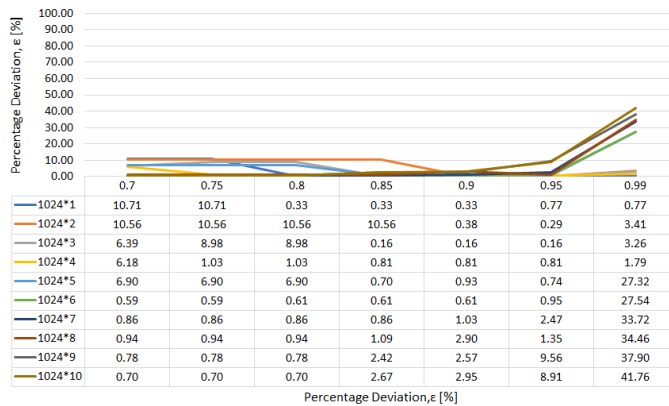
(a)

Second Mode of Six –Storey Shear Frame



(b)

Third Mode of Six –Storey Shear Frame



(c)

Figure 12. Percentage deviation (error) of modal damping ratio for the high damped six-storey frame (5%): (a) the first mode; (b) second mode; (c) the third mode

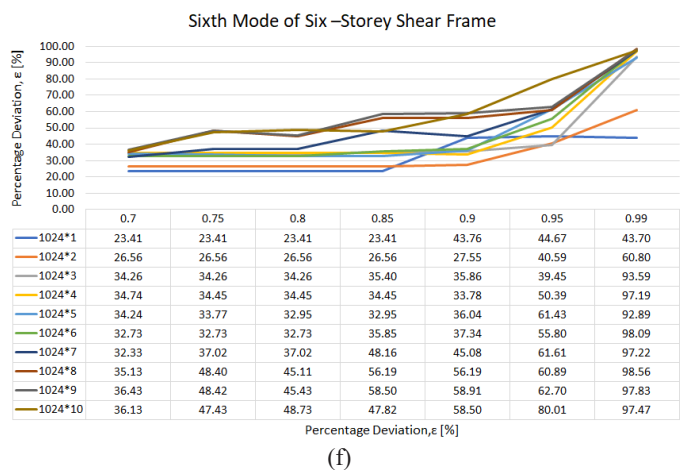
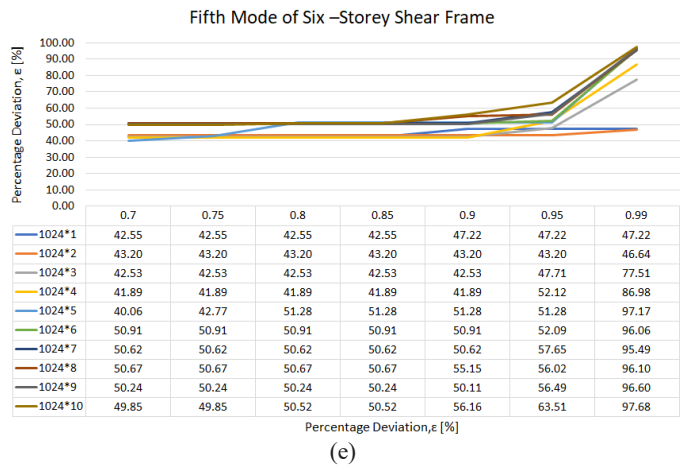
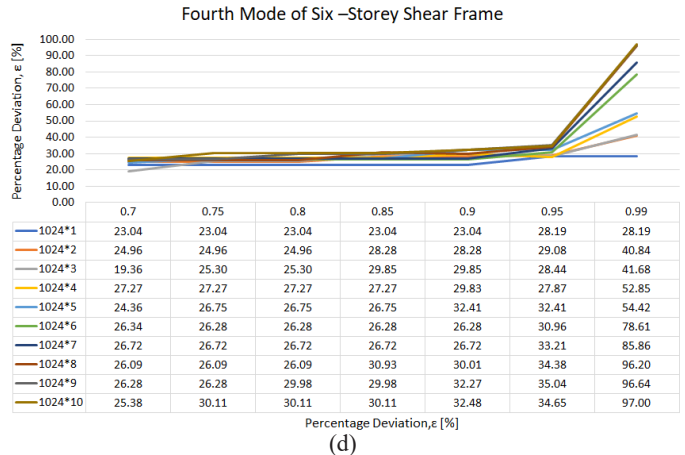


Figure 12. Percentage deviation (error) of modal damping ratio for the high damped six-storey frame (5%): (d) the fourth mode; (e) the fifth mode; (f) the sixth mode.

correlation is adequate and able to successfully capture all full modal decay that contains an adequate amount of information about the decaying CF, otherwise the likely presence of noise and errors in the results for the modal damping estimate will be caused by the spectral estimation. Since the identification of the modal damping ratio using logarithmic decrement is fully reliant on modal decay, the accurate maximum number of time segment lengths becomes a crucial step for accurate estimation of the modal parameter. The results of this analysis for the percentage deviation of the estimated modal damping ratio are illustrated in Figures 4 to 12.

Meanwhile, results of theoretical modal decay of the first mode and limits of the auto-correlation functions calculated using the time segment lengths defined in Table 2 for two, three and six-storey frame are shown in Figures 13, 14 and 15.

This is proven with the scheme presented in Figure 13, 14 and 15, which display the theoretical modal decay of the first mode and the limits of the auto-correlation functions calculated using the time segment lengths defined in Table 2 for multi-storey shear-type models and a variable level of damping (1%, 3% and 5% of critical damping, which consists of low and high damped systems). The red vertical lines that are clearly observed before the end of the decay, consequently, lead to the bias estimates. The effect of the introduced errors can also be observed by comparing, for instance, the auto-correlation estimated using time segments with 2048 points (Figure 16 with its theoretical counterpart Figure 14a): the estimated decay vanishes just at the end of the estimated segment, approximately at 5 seconds or 6 seconds, but the estimated correlation does not contain some points after the

Table 2
Scenarios for the application of the FDD method

| Maximum number of points in the time segments | MAC Index | | | | | | |
|---|-----------|------|------|------|------|------|------|
| | 0.70 | 0.75 | 0.80 | 0.85 | 0.90 | 0.95 | 0.99 |
| 1024*1 | 1a | 1b | 1c | 1d | 1e | 1f | 1g |
| 1024*2 | 2a | 2b | 2c | 2d | 2e | 2f | 2g |
| 1024*3 | 3a | 3b | 3c | 3d | 3e | 3f | 3g |
| 1024*4 | 4a | 4b | 4c | 4d | 4e | 4f | 4g |
| 1024*5 | 5a | 5b | 5c | 5d | 5e | 5f | 5g |
| 1024*6 | 6a | 6b | 6c | 6d | 6e | 6f | 6g |
| 1024*7 | 7a | 7b | 7c | 7d | 7e | 7f | 7g |
| 1024*8 | 8a | 8b | 8c | 8d | 8e | 8f | 8g |
| 1024*9 | 9a | 9b | 9c | 9d | 9e | 9f | 9g |
| 1024*10 | 10a | 10b | 10c | 10d | 10e | 10f | 10g |

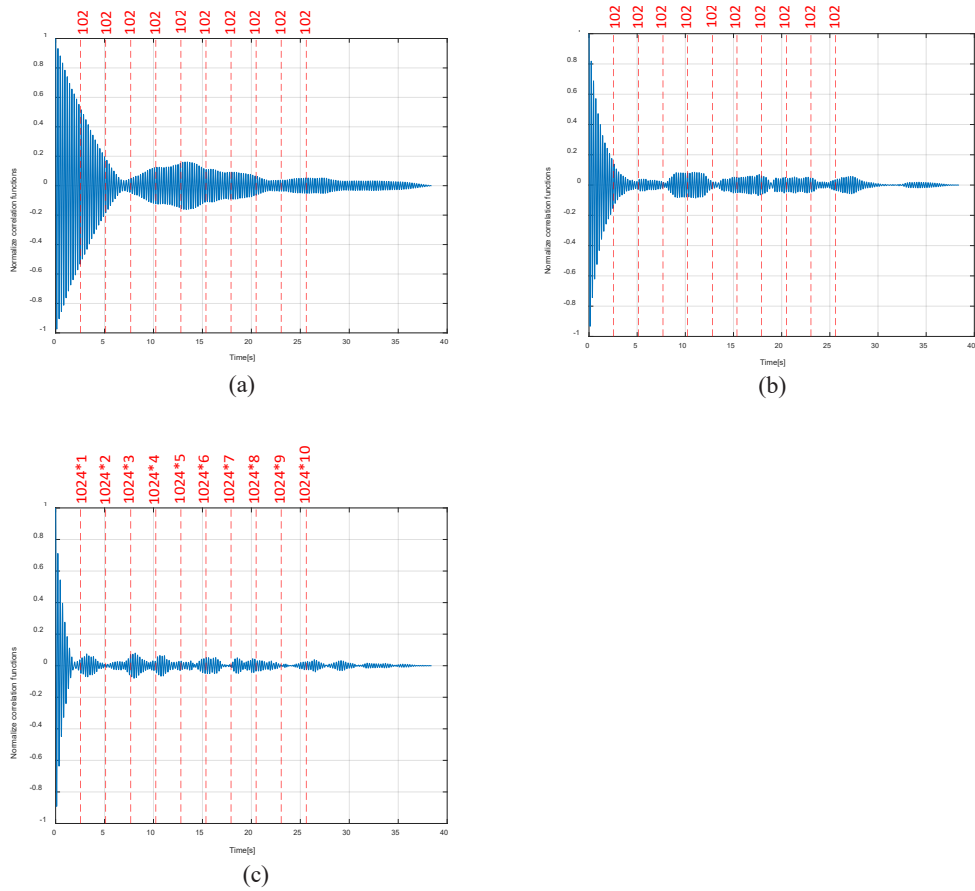


Figure 13. Theoretical modal decay of the first mode and limits of the auto-correlation functions calculated using the time segment lengths defined in Table 2 for two-storey frame: (a) low damped (1%); (b) high damped (3%); (c) high damped (5%) system.

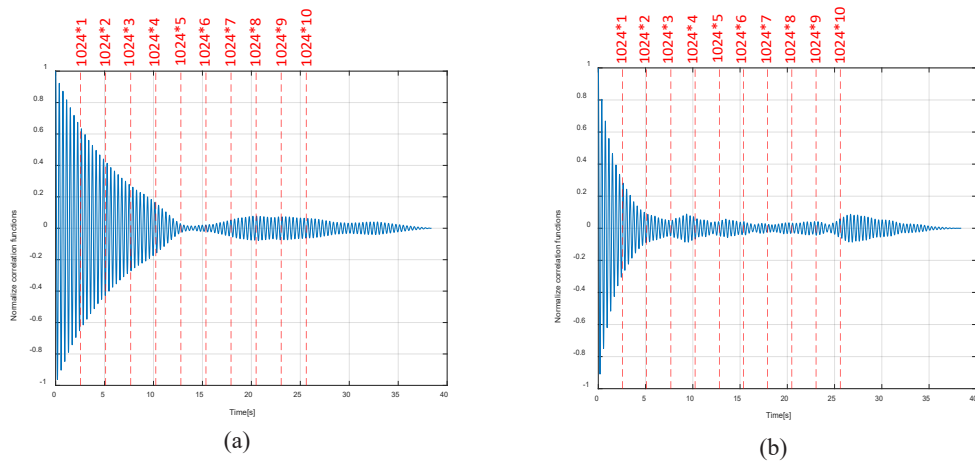
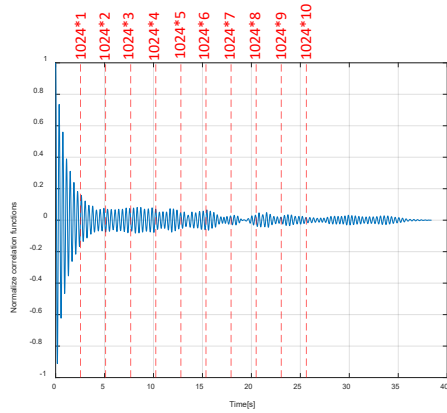


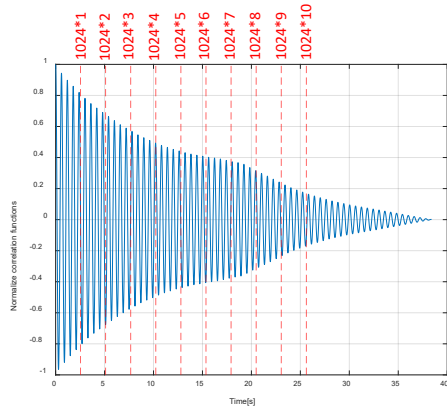
Figure 14. Theoretical modal decay of the first mode and limits of the auto-correlation functions calculated using the time segment lengths defined in Table 2 for three-storey frame: (a) low damped (1%); (b) high damped (3%)

Parameters Study That Effect the Estimated Modal Parameters

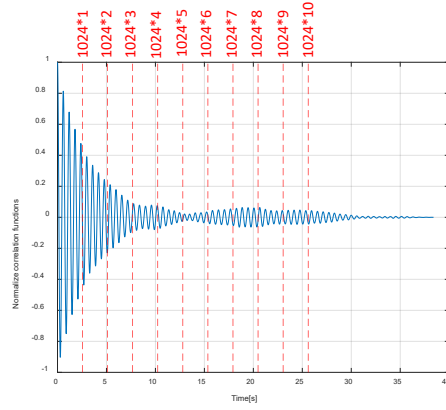


(c)

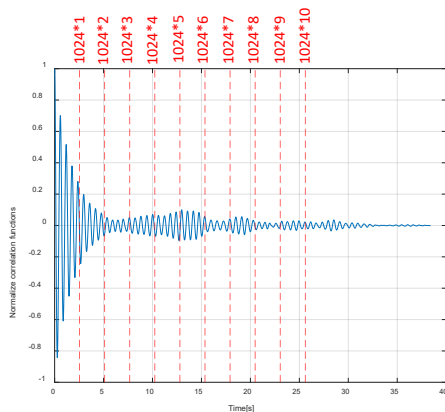
Figure 14. Theoretical modal decay of the first mode and limits of the auto-correlation functions calculated using the time segment lengths defined in Table 2 for three-storey frame: (c) high damped (5%) system



(a)



(b)



(c)

Figure 15. Theoretical modal decay of the first mode and limits of the auto-correlation functions calculated using the time segment lengths defined in Table 2 for six-storey frame: (a) low damped (1%); (b) high damped (3%); (c) high damped (5%) system.

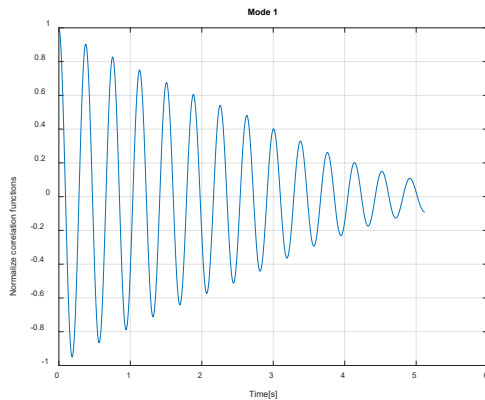


Figure 16. Modal decay estimated using time segments with 2048 points for the first mode of the three-storey frame (1% of critical damping)

disappearance of the decay. This indicates that the length of the estimated correlation is not long enough to characterise the full decay.

In the case of the various levels of damping of the system, the appropriate maximum number of points of the time segment become a crucial decision and need to be defined properly, particularly for low damped systems where the response will decay at a slower rate and thus requiring the high number of points of time segments when compared to a high damped structure. Table 3 provides the appropriate adopted number of points of time segments for the first mode of the multi-storey frame based on the results provided in Figures 4 to 12. The first mode becomes a key point to determine the maximum number of points of the time segments. This has proven that the accurate selection of the time segment length does not rely solely on modal damping ratios; instead, natural frequencies also need to be taken into account because each first mode of multi-storey shear-type models has a different value of natural frequencies. This indicates that reducing the value of natural frequencies and modal damping ratios of the modes under analysis demands longer time segments and a high value of the maximum number of points for an adequate amount of information of the decaying CF when estimating modal damping (examples are shown in Figure 6a and Figure 15a for the first the mode of the six-storey shear model with 1% of critical damping). Furthermore, if the maximum number of points of the time segment is too high, it will cause bias errors. Thus, from this analysis, the maximum number of points of the time segment suitable to be used for both low and high damped systems (1%–5% of critical damping and from frequency 1.5 Hz and above) for multi-storey shear-type models is 5120 (1024×5) or more, as outlined in Table 3. Instead of an increasing number of points of time segments, another way to enhance the frequency resolution is through interpolation of the spectrum by zero-padding the time window to increase the length of recordings (Ewins, 2000).

Table 3

The appropriate adopted number of points of time segments for the multi-storey frame

| Storey frame | Natural frequency [Hz] | Modal damping ratio [%] | Appropriate no. of point of time segments |
|--------------|------------------------|-------------------------|---|
| Two | 4.211 | 1 | $\geq 1024*3 @ (3072)$ |
| | | 3 | $\geq 1024*1 @ (1024)$ |
| | | 5 | $\geq 1024*1 @ (1024)$ |
| Three | 2.657 | 1 | $\geq 1024*4 @ (4096)$ |
| | | 3 | $\geq 1024*2 @ (2048)$ |
| | | 5 | $\geq 1024*1 @ (1024)$ |
| Six | 1.666 | 1 | $\geq 1024*5 @ (5120)$ |
| | | 3 | $\geq 1024*3 @ (3072)$ |
| | | 5 | $\geq 1024*2 @ (2048)$ |

In addition, the supplementary set of analysis involving the parameters of the MAC index with different levels of system damping and the number of points of the time segments revealed that the results yield small variations of the percentage deviation of the modal damping ratio (around 1.23% standard deviation) for multi-storey shear-type models with 1% (low damped system) as shown in Figures 4, 5 and 6. This proves that the MAC index does not significantly affect the results of the low damped system. The use of a high MAC index value for the high damped system (5% of critical damping) will significantly introduce large error bound about 8.71% standard deviation of percentage error. It became worse, particularly for the higher modes, as the standard deviation of percentage error increased gradually. Furthermore, the use of a MAC index for a high number of points of time segments significantly increases the standard deviation of the percentage error. The plots in Figures 7 to 12 also revealed that the use of a high number of points of time segments as well as a high MAC index lead to an increased percentage deviation of estimate modal damping ratio, which can be up to 30% of standard deviation when the level of damping is higher. The selection of the auto-spectra based on the MAC index using values higher than 0.8 is preferred by most researchers (Magalhães, 2010; Magalhães et al., 2010) but it is unsuitable, particularly for the higher modes of the high damped system.

Therefore, this analysis also provides the appropriate range for the MAC index for each mode with different levels of damping according to the trend, as illustrated in Figure 4 to 12. The results of the analysis are provided in Tables 4, 5 and 6 with respect to two-, three- and six-storey frames. Table 7 comprises all the appropriate range of MAC indexes with different levels of damping from multi-storey models according to each mode, based on the results in Figures 4 to 12. This Table 7 clearly shows that the higher modes require lower MAC index values and vice versa for lower modes.

Table 4

The appropriate adopted range of MAC index for the two-storey frame

| Mode | Natural frequency [Hz] | Modal damping ratio [%] | Appropriate MAC index |
|--------|------------------------|-------------------------|-----------------------|
| First | 4.211 | 1 | 0.70–0.90 |
| | | 3 | 0.80–0.99 |
| | | 5 | 0.70–0.95 |
| Second | 10.911 | 1 | 0.70–0.95 |
| | | 3 | 0.70–0.90 |
| | | 5 | 0.70–0.85 |

Table 5

The appropriate adopted range of MAC index for the three-storey frame

| Mode | Natural frequency [Hz] | Modal damping ratio [%] | Appropriate MAC index |
|--------|------------------------|-------------------------|-----------------------|
| First | 2.657 | 1 | 0.75–0.99 |
| | | 3 | 0.70–0.99 |
| | | 5 | 0.85–0.99 |
| Second | 7.445 | 1 | 0.80–0.99 |
| | | 3 | 0.85–0.95 |
| | | 5 | 0.70–0.85 |
| Third | 10.759 | 1 | 0.70–0.90 |
| | | 3 | 0.70–0.90 |
| | | 5 | 0.70–0.75 |

Table 6

The appropriate adopted range of MAC index for the six-storey frame

| Mode | Natural frequency [Hz] | Modal damping ratio [%] | Appropriate MAC index |
|--------|------------------------|-------------------------|-----------------------|
| First | 1.666 | 1 | 0.70–0.90 |
| | | 3 | 0.70–0.90 |
| | | 5 | 0.70–0.95 |
| Second | 4.672 | 1 | 0.70–0.99 |
| | | 3 | 0.70–0.95 |
| | | 5 | 0.70–0.80 |
| Third | 7.448 | 1 | 0.70–0.95 |
| | | 3 | 0.70–0.95 |
| | | 5 | 0.70–0.95 |

Table 6 (Continued)

| Mode | Natural frequency [Hz] | Modal damping ratio [%] | Appropriate MAC index |
|--------|------------------------|-------------------------|-----------------------|
| Fourth | 9.789 | 1 | 0.70–0.99 |
| | | 3 | 0.70–0.90 |
| | | 5 | 0.70–0.85 |
| Fifth | 11.587 | 1 | 0.70–0.99 |
| | | 3 | 0.70–0.95 |
| | | 5 | 0.70–0.75 |
| Sixth | 13.082 | 1 | 0.70–0.95 |
| | | 3 | 0.70–0.75 |
| | | 5 | 0.70–0.85 |

Table 7

The appropriate adopted range of MAC index for each mode

| Mode | Modal damping ratio [%] | Appropriate Range of MAC index | Appropriate MAC index |
|--------|-------------------------|--------------------------------|-----------------------|
| First | 1 | 0.75–0.90 | |
| | 3 | 0.80–0.90 | 0.85–0.90 |
| | 5 | 0.85–0.95 | |
| Second | 1 | 0.80–0.95 | |
| | 3 | 0.85–0.90 | 0.85–0.90 |
| | 5 | 0.70–0.80 | |
| Third | 1 | 0.70–0.90 | |
| | 3 | 0.70–0.90 | 0.70–0.75 |
| | 5 | 0.70–0.75 | |
| Fourth | 1 | 0.70–0.99 | |
| | 3 | 0.70–0.90 | 0.70–0.85 |
| | 5 | 0.70–0.85 | |
| Fifth | 1 | 0.70–0.99 | |
| | 3 | 0.70–0.95 | 0.70–0.75 |
| | 5 | 0.70–0.75 | |
| Sixth | 1 | 0.70–0.95 | |
| | 3 | 0.70–0.75 | 0.70–0.75 |
| | 5 | 0.70–0.85 | |

CONCLUSIONS

In this study, the results of the parameters that have a bigger effect on the performance of the automated EFDD method are presented involving the maximum number of points considered in the time segments used for the spectra calculation, selection of MAC index and the variable level of damping of the system. The results indicate that reducing the value of natural frequencies and modal damping ratios of the modes under analysis demands longer time segments and a high value of the maximum number of points for adequate information of the decaying CF when estimating modal damping. In addition, the supplementary set of analyses involving the parameters of the MAC index with different levels of system damping and number of points of the time segments revealed that the results proved that the MAC index did not significantly affect the results for the low damped system. However, the use of a high MAC index value for the high damped system (5% of critical damping) significantly introduced large error bound. It became worse, particularly for the higher modes, as the standard deviation of percentage error increased gradually. Furthermore, the use of a MAC index for a high number of points of time segments significantly increased the standard deviation of the percentage error. Therefore, a careful treatment of a maximum number of points of time segments and MAC index numbers regarding the variable level of system damping and degree of freedom of the system are an important element in achieving an accurate estimate of modal parameters. Therefore, the attempted simulations have confirmed the efficacy of the implemented analysis. This research serves as a base for future studies in enhancing the performance of the automated EFDD method as a modal information engine in structural health monitoring (SHM) systems by providing a better choice of a maximum number of points of time segments and MAC index number regarding the variable level of system damping and degree of freedom of the system.

ACKNOWLEDGMENTS

The authors would like to extend their greatest gratitude to the Institute of Noise and Vibration UTM for funding the current study under the Higher Institution Centre of Excellence (HICoE) Grant Scheme (R.K130000.7843.4J227 and R.J130000.7824.4J234). Additional funding for this research came from the UTM Research University Grant (Q.K130000.2543.11H36) and the Fundamental Research Grant Scheme (R.K130000.7840.4F653) from The Ministry of Higher Education, Malaysia.

REFERENCES

- Bajrić, A., Georgakis T. C., & Brincker, R. (2015a, February 2-5). Evaluation of damping using frequency domain operational modal analysis techniques. In *Proceedings of the 33rd International Modal Analysis Conference* (pp. 351-355). Orlando, USA.

- Bajric, A., Brincker, R., & Thöns, S. (2015b, May 12-14). Evaluation of damping estimates in the presence of closely spaced modes using operational modal analysis techniques. In *Proceedings of the 6th International Operational Modal Analysis Conference* (pp. 1-13). Gijon, Spain.
- Brewick, P. T., & Smyth, A. W. (2013). An investigation of the effects of traffic induced local dynamics on global damping estimates using operational modal analysis. *Mechanical Systems and Signal Processing*, *41*(1-2), 433-453.
- Bricker, R., & Venture, C. (2015). *Introduction to operational modal analysis*. Chichester, England: John Wiley and Sons, Ltd.
- Brincker, R., Ventura, C. E., & Andersen, P. (2001a, February 5-8). Damping estimation by frequency domain decomposition. In *Proceedings of the 19th International Modal Analysis Conference* (pp. 698-703). Hyatt Orlando, USA.
- Brincker, R., Zhang, L., & Andersen, P. (2001b). Modal identification of output-only systems using frequency domain decomposition. *Smart Materials and Structures*, *10*(3), 441-445.
- Brincker, R., & Zhang, L. (2009, May 4-6). Frequency domain decomposition revisited. In *Proceedings of the 3rd International Operational Modal Analysis Conference* (pp. 615-626). Portonovo, Italy.
- Chopra, A. K. (2001). *Dynamics of Structures: Theory and applications to earthquake engineering*. New Jersey, USA: Prentice Hall
- Chou, J. Y., & Chang, C. M. (2020). Modal property extraction based on frequency domain stochastic subspace identification. In *Proceedings of the 13th International Conference on Damage Assessment of Structures* (pp. 303-313). Singapore: Springer.
- Ewins, D. J. (2000). *Modal testing: Theory, practice, and application*. Hertfordshire, England: Research Studies Press.
- Frans, R., & Arfiadi, Y. (2019). Structural system identification of plane frames based on frequency domain decomposition-natural excitation technique (FDD-NExT). *IOP Conference Series: Materials Science and Engineering*, *615*(1), 1-10.
- Gade, S., Møller, N. B., Herlufsen, H., & Konstantin-Hansen, H. (2005, April 26-27). Frequency domain techniques for operational modal analysis. In *Proceedings of the 1st International Operational Modal Analysis (IOMAC) Conference* (pp. 261-271). Copenhagen, Denmark.
- Ghalishooyan, M., Shooshtari, A., & Abdelghani, M. (2019). Output-only modal identification by in-operation modal appropriation for use with enhanced frequency domain decomposition method. *Journal of Mechanical Science and Technology*, *33*(7), 3055-3067.
- Hwang, J. S., Kwon, D. K., & Kareem, A. (2019). Frequency domain state space-based mode decomposition framework. *Journal of Engineering Mechanics*, *145*(7), 1-45.
- Jacobsen, N., Andersen, P., & Bricker, R. (2008, February 4-7). Applications of frequency domain curve-fitting in the EFDD technique. In *Proceedings of the 26th International Modal Analysis Conference* (pp. 1-13). Orlando, Florida.
- Magalhães, F. (2010). *Operational modal analysis for testing and monitoring of bridges and special structures* (PhD Thesis). University of Porto, Portugal.

- Magalhães, F., Cunha, Á., Caetano, E., & Brincker, R. (2010). Damping estimation using free decays and ambient vibration tests. *Mechanical Systems and Signal Processing*, 24(5), 1274-1290.
- Mironov, A., Doronkin, P., Priklonsky, A., & Kabashkin, I. (2015). Condition monitoring of operating pipelines with operational modal analysis application. *Transport and Telecommunication Journal*, 16(4), 305-319.
- Pioldi, F. (2012). *Sulla stima dello smorzamento modale mediante algoritmo frequency domain decomposition* [On the estimation of modal damping by frequency domain decomposition algorithm] (BSc. Thesis). Università di Bergamo, Italy.
- Pioldi, F. (2013). *Sulla formulazione di algoritmi ottimizzati di identificazione dinamica modale e loro applicazione in ambito sismico* [On the formulation of optimized modal dynamic identification algorithms and their application in seismic fields] (MSc. Thesis). University of Bergamo, Italy.
- Pioldi, F., Ferrari, R., & Rizzi, E. (2014, September 15-17). A refined FDD algorithm for operational modal analysis of buildings under earthquake loading. In *Proceedings of the 26th International Conference on Noise and Vibration Engineering* (pp. 3353-3368). Leuven, Belgium.
- Pioldi, F., Ferrari, R., & Rizzi, E. (2016). Output-only modal dynamic identification of frames by a refined FDD algorithm at seismic input and high damping. *Mechanical Systems and Signal Processing*, 68, 265-291.
- Pioldi, F., Ferrari, R., & Rizzi, E. (2017). Earthquake structural modal estimates of multi-storey frames by a refined Frequency Domain Decomposition algorithm. *Journal of Vibration and Control*, 23(13), 2037-2063.
- Pioldi, F., & Rizzi, E. (2015, September 14-17). On modal identification of structures from earthquake response signals by a refined frequency domain decomposition approach. In *Proceedings of the 22nd Conference of the Associazione Italiana Di Meccanica Teorica E Applicata (AIMETA 2015)* (pp. 307-316). Genova, Italy.
- Pioldi, F., & Rizzi, E. (2017). A refined frequency domain decomposition tool for structural modal monitoring in earthquake engineering. *Earthquake Engineering and Engineering Vibration*, 16(3), 627-648.
- Pioldi, F., & Rizzi, E. (2018). Earthquake induced structural response output only identification by two different operational modal analysis techniques. *Earthquake Engineering and Structural Dynamics*, 47(1), 257-264.
- Rainieri, C., & Fabbrocino, G. (2014). *Operational modal analysis of civil engineering structures*. New York, NY: Springer.
- Rainieri, C., & Fabbrocino, G. (2015, May 12-14). Learning operational modal analysis in four steps. In *Proceeding of the 6th International Operational Modal Analysis Conference* (pp. 1-12). Gijón, Spain.
- Rodrigues, J., Brincker, R., & Andersen, P. (2004, January 26-29). Improvement of frequency domain output-only modal identification from the application of the random decrement technique. In *Proceedings of the 23rd International Modal Analysis Conference* (pp. 92-100). Dearborn, Michigan, USA.
- Tarinjad, R., & Damadipour, M. (2014). Modal identification of structures by a novel approach based on FDD-wavelet method. *Journal of Sound and Vibration*, 333(3), 1024-1045.

- Wang, T., Zhang, L., & Tamura, Y. (2005). An operational modal analysis method in frequency and spatial domain. *Earthquake Engineering and Engineering Vibration*, 4(2), 295-300.
- Zanchi, D. Z. (2011). *Identificazione dinamica modale di strutture mediante tecniche basate sul solo segnale di risposta* [Dynamic modal identification of structures using techniques based on the response signal only] (MSc. Thesis). Università di Bergamo, Italy.
- Zhang, L., Brincker, R., & Andersen, P. (2005, April 26-27). An overview of operational modal analysis: Major development and issues. In *Proceedings of the 1st International Operational Modal Analysis Conference* (pp. 179-190). Copenhagen, Denmark.
- Zhang, L., & Tamura, Y. (2003, September 16-18). Damping estimation of engineering structures with ambient response measurements. In *Proceedings of the 21st International Modal Analysis Conference* (pp. 226-233). Kissimmee, Florida.
- Zhang, L., Wang, T., & Tamura, Y. (2010). A frequency-spatial domain decomposition (FSDD) method for operational modal analysis. *Mechanical Systems and Signal Processing*, 24(5), 1227-1239.

APPENDIX

Nomenclature list

| | |
|--------|--------------------------------------|
| FDD | Frequency Domain Decomposition |
| SDOF | Single Degree of Freedom |
| MAC | Modal Assurance Criterion |
| SSI | Stochastic Subspace-Based Algorithms |
| OMA | Operational Modal Analysis |
| EMA | Experimental Modal Analysis |
| SVD | Singular Value Decomposition |
| PSD | Power Spectrum Density |
| LogDec | Logarithmic Decrement |
| HT | Hilbert Transform |
| NExt | Natural Excitation Techniques |
| CF | Correlation Function |
| SD | Spectral Density |
| SHM | Structural Health Monitoring |
| RUL | Remaining Useful Life |
